Hsa-miR-23a-5p: A Potential Prognostic Biomarker in Diffuse Large B-cell Lymphoma

Yunfei Zhao[1], Anna Su[1], Rui Bai[2], Gulimire Adili[1], Laxin Sabitjan[1], and Xun Li[1]

[1] *Department of Oncology, The Fourth Clinical Medical College of Xinjiang Medical University, Urumqi, China*
[2] *Health Management Center, People's Hospital of Xinjiang Uygur Autonomous Region, Urumqi, China*

ABSTRACT

This study aimed to identify a novel microRNA (miRNA)-related circulating biomarker that is easily accessible for clinical use and can dynamically monitor the biological characteristics of diffuse large B-cell lymphoma (DLBCL).

We analyzed miRNA expression profiles in DLBCL from the Gene Expression Omnibus (GEO) (GSE171272 and GSE173080) and The Cancer Genome Atlas (TCGA). The immune microenvironment and immune-related gene differences associated with hsa-miR-23a-5p were assessed through the single-sample gene set enrichment analysis and CIBERSORT. Gene set enrichment analysis identified expression trends related to hsa-miR-23a-5p. The 50% inhibitory concentration of chemotherapy agents was estimated for hsa-miR-23a-5p. Potential miRNA targets were identified using TargetScan, miRWalk, and RNA22, and validated with miRTarBase, DIANA-TarBase, and NPInter. Gene functions and associated pathways were analyzed through Gene Ontology and the Kyoto Encyclopedia of Genes and Genomes. Protein-Protein Interaction networks were built using Cytoscape. *SNRPD1*-related analysis was conducted using TCGA and GEO data.

Hsa-miR-23a-5p was significantly overexpressed in the tumor tissues and serum exosomes of patients with DLBCL. The expression levels of hsa-miR-23a-5p were associated with distinct prognostic outcomes, immune landscapes, chemoresistance, and biological processes, serving as potential risk factors. The target gene *SNRPD1* was an independent prognostic factor significantly associated with patient survival.

This study identifies hsa-miR-23a-5p and its target *SNRPD1* as potential prognostic factors for DLBCL. Specifically, the overexpression of hsa-miR-23a-5p in serum exosomes of patients with DLBCL suggests that it could serve as a convenient, non-invasive biomarker for clinical evaluation of DLBCL. However, further research and validation are necessary to confirm these findings.

Keywords: Diffuse large B-cell lymphoma; Exosome; MicroRNA; Prognosis

INTRODUCTION

Diffuse large B-cell lymphoma, not otherwise specified (DLBCL, NOS) is the most prevalent classification of large B-cell lymphoma, accounting for 30% of all cases of non-Hodgkin lymphoma.[1] This study

---

Corresponding Author: Xun Li, PhD;
Department of Oncology, The Fourth Clinical Medical College of Xinjiang Medical University, Urumqi, 830002, China. Tel: (+86) 135 7981 8166, Email: 1984661032@qq.com

primarily focused on DLBCL (NOS), hereafter referred to simply as DLBCL. DLBCL is a heterogeneous and aggressive disease, with significant variations in clinical presentation, pathological characteristics, molecular markers, treatment, and prognosis.[1–7] The incidence of DLBCL is 5.5 per100 000, according to the US cancer registry.[8] Although the R-CHOP regimen (rituximab, cyclophosphamide, vincristine, doxorubicin, and prednisolone) cures a substantial proportion of patients with DLBCL as a first-line treatment, approximately 10% to 15% of patients present with refractory disease, while 20% to 25% relapse, usually within the first 2 years.[9–12] Among patients with relapsed/refractory DLBCL, only approximately 10% can be cured with autologous hematopoietic stem cell transplantation and salvage chemotherapy regimens.[13–15] This underscores the need for improved treatment strategies in DLBCL and highlights the importance of risk stratification, laying the groundwork for more targeted and personalized therapies. DLBCL risk assessment predominantly relies on the International Prognostic Index (IPI) and the cell of origin (COO) classification, which classifies DLBCL into two subtypes: germinal center B-cell-like (GCB) and activated B-cell-like (ABC). Nonetheless, the IPI and COO have faced challenges in their application to risk stratification for some cases, as the COO-based distinction does not fully account for the heterogeneity of DLBCL and its response to chemotherapy, and they do not accurately predict clinical outcomes.[16] In recent years, the discovery and detection of microRNAs (miRNAs) have brought new hope for the risk stratification of DLBCL.

MiRNAs are small non-coding RNA molecules, usually 17 to 25 nucleotides in length, that are essential in regulating gene expression and have significant implications in the initiation and progression of cancer.[17] Research indicates that miRNAs play a crucial role in regulating essential cellular processes, influencing apoptosis, development, and proliferation, by modulating the expression of target mRNAs at the post-transcriptional level.[18,19] They display unique expression patterns in cancer tissues, which vary across different cancer types, making miRNAs promising tools for both cancer diagnosis and therapy.[17] MiRNAs are produced by various cells within the tumor microenvironment and, upon release, circulate in body fluids. Typically, they are encapsulated in protective exosomes, which shield them from enzymatic degradation.[20] Since 1996, the biological relevance of exosomes and their capacity to deliver antigens has been increasingly emphasized.[21] Among the RNAs in plasma-derived exosomes, miRNAs are the most prevalent and significantly influence cancer progression by accelerating tumor growth and promoting an immunosuppressive microenvironment.[22,23]

Exosomes are vesicles secreted by living cells, and their specific molecular profiles can be used to evaluate tumor biological status.[24] However, there is limited prospective research on the effectiveness of quantitative or qualitative exosome analysis as an indicator for DLBCL. This research aimed to evaluate the significance of miRNAs within the DLBCL microenvironment and to screen for potential serum exosome-derived miRNAs associated with DLBCL status, thereby providing a basis for developing a non-invasive liquid biopsy strategy for clinical assessment.

MATERIALS AND METHODS

Dataset Origin and Selection

The datasets GSE185796, GSE171272, GSE173080, GSE117063, GSE21849, GSE42906, and GSE12933 were sourced from the open-access Gene Expression Omnibus (GEO) database hosted by the National Center for Biotechnology Information (https://www.ncbi.nlm.nih.gov/). The selection criteria for the DLBCL datasets were as follows: (a) miRNA detection in exosomes or tissues, (b) inclusion of normal tissue control groups, and (c) datasets with more than 1000 detected miRNA species.

Based on these criteria, the DLBCL datasets GSE173080 and GSE171272 were selected for the analysis of differentially expressed miRNAs. The dataset GSE173080, based on the GPL25134 Platform (Agilent-070156 Human miRNA V21.0 Microarray; ID 046064), contained miRNA expression profiles from DLBCL (untreated patients) tumor tissues and control groups (lymph node reactive hyperplasia, LRH) comprising 10 samples [tumor group (n=5) and control group (n=5)]. The dataset GSE171272, utilizing the GPL18058 Platform, specifically the Exiqon miRCURY LNA miRNA array (7th gen-miRBase v18), contained serum exosomal miRNAs from patients with DLBCL (untreated patients) and healthy controls in 15 samples [tumor group (n=10) and control group (n=5)]. All data from GSE173080 and GSE171272 were normalized. The GSE173080 dataset was processed with quantile normalization, while the GSE171272 dataset underwent

the median Normalization method for normalization. The limma package (version 3.62.2) was employed to identify differentially expressed miRNAs, applying a filter of adjusted $p<0.05$ & |logFC|>1.5. The dbDEMC database (https://www.biosino.org/dbDEMC/) was used to present the differential expression of miRNAs across various tumor types compared to normal tissues. The expression values of dbDEMC were log2-transformed (base 2) and subsequently normalized using quantile normalization.

Transcriptomic Expression Analysis in the TCGA

The TCGA database portal (https://portal.gdc.cancer.gov/) is a comprehensive source of information on cancer genes, including tumor tissue DNA, mRNA gene expression, and miRNA expression profiling, along with the relevant clinical data. A total of 47 specimen datasets from DLBCL patients were downloaded. For the mRNA data, Transcripts Per Million (TPM) was used for normalization, followed by a $\log_2$ (TPM+1) transformation. For miRNA data, reads per million (RPM) normalization was applied. To gain deeper insights into the tumor microenvironment and characteristics in DLBCL patients, survival (version 3.8-3), xCell (version 1.1.0), GSVA (version 1.50.1), timeROC (version 0.4), corrplot (version 0.95), gene set enrichment analysis (GSEA) (version 1.68.0), oncoPredict (version 1.2), and maftools (version 2.22.0) packages were used to perform various analyses including survival, immune cell type enrichment, single-sample gene set enrichment analysis, time-dependent receiver operating characteristic (ROC) curves, correlation, gene set enrichment, inhibitory concentration 50% (IC_{50}), and gene mutation analysis, respectively.

Targeted Gene Screening and Analysis

The databases used for predicting miRNA targets, TargetScan (https://www.targetscan.org/vert_80/), miRWalk (http://mirwalk.umm.uni-heidelberg.de/), and RNA22 (https://cm.jefferson.edu/rna22/) were used to identify miRNA target genes. Gene Ontology (GO) and Kyoto Encyclopedia of Genes and Genomes (KEGG) enrichment analyses were conducted using the clusterProfiler package. The protein-protein interaction (PPI) networks were constructed with Cytoscape software (Version 3.10.2) plug-in unit stringAPP (Version 2.1.1), MCODE (Version 2.0.3), and cytoHubba (Version 0.1), applying algorithms such as Maximum Neighborhood Component (MNC), Density

of Maximum Neighborhood Component (DMNC), Maximal Clique Centrality (MCC), and Degree to uncover key hub genes. The databases of miRNA-target interactions confirmed by experimentation, miRTarBase (https://mirtarbase.cuhk.edu.cn/), DIANA-TarBase (http://diana.imis.athena-innovation.gr/), and NPInter (http://bigdata.ibp.ac.cn/npinter4) were utilized to confirm miRNA target genes.

Survival Analysis and Clinical Characteristics

The GSE31312 dataset, based on the GPL570 platform (Affymetrix U133 Plus 2.0 Array), includes mRNA expression profiles from DLBCL tumor tissues and associated clinical data, such as sex, age, disease stage, COO type, IPI score, serum lactate dehydrogenase (LDH) level, Eastern Cooperative Oncology Group (ECOG) performance, and B-symptoms. This dataset underwent normalization using quantile normalization. All clinicopathological factors were categorized based on the IPI criteria. Survival analysis, and univariate and multivariate Cox proportional hazards regression, was performed using the survival package in R to assess risk factors.

Statistical Analysis

All statistical analyses were conducted using SPSS (version 27.0) and R (version 4.4.1). Chi-square, Fisher's exact, and Kruskal-Wallis rank-sum test was employed to compare patient characteristics. The relationship between trends in two groups was evaluated using the Chi-square test for independence. The median expression value was used as the threshold to categorize samples into low- and high-expression groups. Overall survival (OS) was assessed starting at diagnosis until death from any cause. The Benjamini-Hochberg method was applied to control the false discovery rate and to compute the adjusted p value for the differentially expressed miRNAs in the GSE173080 and GSE171272 datasets, as well as for the enriched gene sets in the HALLMARK collection and the KEGG and GO analysis. All statistical tests were two-tailed, with a significance level of $p<0.05$.

RESULTS

MiRNA Expression in DLBCL Tumor Tissues and Serum Exosomes

MiRNA expression profiles from the GSE173080 and GSE171272 datasets were analyzed to identify

differentially expressed miRNAs in DLBCL tumor tissues and serum exosomes, respectively (Supplementary Tables 1 and 2). In the GSE173080 dataset, a box plot of miRNA expression is shown in Figure 1A. The samples GSM5259474 and GSM5259477 were excluded from healthy control group due to abnormal expression. To visualize the differentially expressed miRNAs, a volcano plot was generated (Figure 1C). MiRNAs that met the significance threshold—adjusted $p<0.05$ and |logFC|>1.5—were considered significantly altered (Figure 1E). In total, 35 differentially expressed miRNAs were selected. Similarly, the exosomal miRNA expression profiles from the GSE171272 dataset were analyzed (Figure 1B), and the corresponding volcano plot was shown in Figure 1D. Differentially expressed miRNAs were determined using the same filtering criteria (adjusted $p<0.05$ and |logFC| > 1.5) (Figure 1F).
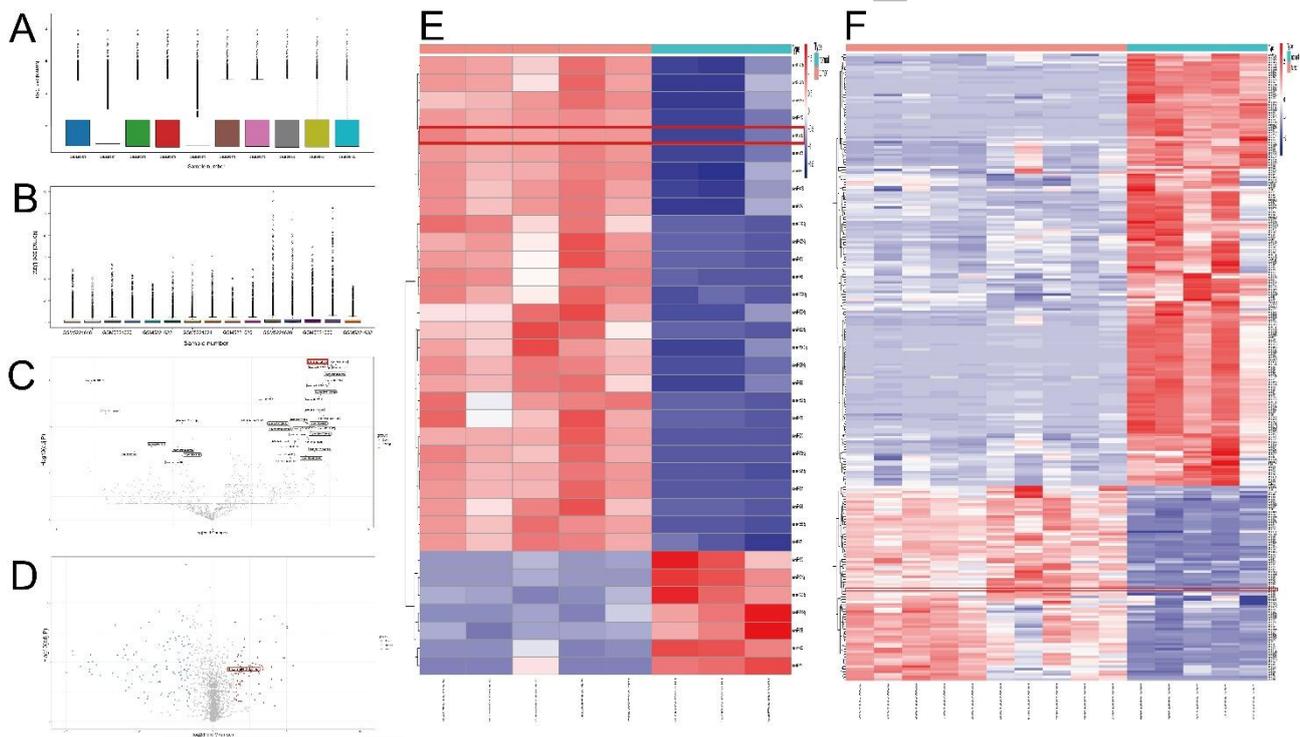

Figure 1. Analysis of differentially expressed miRNAs in tumor tissues and exosomes.
A. Box plot of the GSE173080. B. Box plot of the GSE171272. C. Volcano plot depicting the significantly differentially expressed miRNAs between tissue samples in the GSE173080 dataset. D. Volcano plot depicting the significantly differentially expressed serum exosomal miRNAs in the GSE171272 dataset. E. Heatmap for differentially expressed miRNAs in the GSE173080 dataset were identified using the Linear Model and Empirical Bayes Method, with a significance threshold of adjusted $p<0.05$ and fold-change >1.5 after log2 transformation. The row name of the heatmap is the miRNA name, and the column name is the ID of the samples. F. Heatmap for differentially expressed miRNAs in the GSE171272 dataset were identified using the Linear Model and Empirical Bayes Method, with a significance threshold of adjusted $p<0.05$ and fold-change>1.5 after log2 transformation. The row name of the heatmap is the miRNA name, and the column name is the ID of the samples.

A total of 1739 miRNAs were found to intersect between the GSE171272 and GSE173080 datasets (Figure 2A). A chi-square test for independence revealed a significant association ($p=6.195 \times 10^{-6}$) between the upregulation and downregulation of miRNAs in the two datasets (Figure 2B). The differentially expressed miRNAs from the two datasets were then combined, identifying an overlap of 3 miRNAs (Figure 2C). A univariate Cox analysis was performed using DLBCL patients from the TCGA database, identifying 8 statistically significant miRNAs (Figure 2D). By intersecting the differentially expressed

miRNAs identified in GSE171272 with those that were statistically significant in the univariate Cox regression analysis of DLBCL patients from the TCGA database, we identified the target miRNA as hsa-miR-23a-5p (Figure 2E), which was found to be upregulated in various cancers compared to normal tissues (Figure 2F).

Finally, we used the TCGA database to generate survival and ROC curves for hsa-miR-23a-5p. Clinical information from 47 DLBCL patients with hsa-miR-23a-5p expression data was used for survival analysis (Supplementary Tables 6 and 7). Variables such as age, sex, race, clinical stage, primary therapy outcome, radiation therapy, extranodal involvement, follow-up time, and Ki-67 (MIB-1) status were comparable between groups, with the exception of lactate dehydrogenase (LDH) (Table 1). The differences in LDH levels were attributed to the large amount of missing data. Due to a substantial amount of missing data for LDH (18 patients) and Ki67 (20 patients), these variables were excluded from the multifactorial analyses. Survival analyses were plotted, with a $p=0.006$ for subgroups categorized by high and low levels of hsa-miR-23a-5p expression, which was statistically significant (Figure 2G). Both single- and multi-factor survival analyses were performed (Table 2), and hsa-miR-23a-5p was found to be statistically significant in both single-variable and multiple-variable assessments. To further evaluate the predictive power of hsa-miR-23a-5p, time-dependent ROC curves were generated (Figure 2H). The area under the ROC curve (AUC) for the 4-year survival prediction was 0.846, indicating good discriminatory ability.

Correlation of hsa-miR-23a-5p and tumor-infiltrating immune Cells

To further investigate the relationship between hsa-miR-23a-5p expression and the immune microenvironment, the distribution of tumor-infiltrating immune cell (TIC) subsets was analyzed using the CIBERSORT and xCell algorithms. These analyses included immune cell profiles of 21 and 64 immune cells in DLBCL samples, stratified by the median level of hsa-miR-23a-5p expression (Figure 3A). CIBERSORT analysis, which includes 21 immune cell types, revealed that the expression levels of hsa-miR-23a-5p are associated with activated natural killer (NK) cells and resting mast cells. The proportion of activated NK cells was significantly elevated in the low-expression group compared to the high-expression group, while the

opposite trend was observed for resting mast cells, with a higher proportion in the high-expression group (Figure 3B). The xCell analysis, which includes 64 immune cell types, identified a significant correlation between hsa-miR-23a-5p expression levels and various cell types. The proportion of B cells, CD4+ naive T cells, CD4+ T cells, and Tregs was markedly elevated in the low-expression group in comparison to the high-expression group. Conversely, the proportion of keratinocytes and osteoblasts was significantly higher in the high-expression group relative to the low-expression group. (Figure 3C). To visualize these relationships from the xCell analysis, a correlation heatmap was generated for 64 types of TICs (Figure 3D). Among the 58 immune-related genes, the *BTNL2* gene was notably upregulated in the high-expression group of hsa-miR-23a-5p ($p<0.01$) (Figure 3E). These findings demonstrate that hsa-miR-23a-5p is strongly correlated with immune cells and immune-related molecules within the tumor microenvironment, and may play a crucial role in tumor immune evasion and immune-responses regulation.

Hsa-miR-23a-5p as a Promising Indicator for Tumor Proliferation and Chemotherapeutic Resistance in DLBCL

Given the negative correlation between hsa-miR-23a-5p expression and overall survival in DLBCL patients, GSEA was performed on cohorts stratified by the median hsa-miR-23a-5p expression level (Figure 4A–D). In the high-expression group of hsa-miR-23a-5p, genes were predominantly enriched in cell proliferation-associated pathways, such as MTORC1 signalling, IL6-JAK-STAT3 signalling, MYC signalling, and PI3K-AKT-MTOR signalling pathway. These outcomes suggest that hsa-miR-23a-5p could be a biomarker for the tumor proliferative microenvironment. We also compared the predicted drug sensitivity between the high- and low- hsa-miR-23a-5p expression groups (Figure 4E–J). The results demonstrated that the high-expression group of hsa-miR-23a-5p exhibited higher IC50 values for cisplatin, docetaxel, irinotecan, paclitaxel, vinorelbine, and 5-fluorouracil than the low-expression group. These outcomes suggest that hsa-miR-23a-5p is not only closely associated with the proliferative status of tumors but may also influence chemotherapy response, making it a potential biomarker in treatment stratification.

Figure 2. The landscape of differentially expressed miRNAs in the diffuse large B-cell lymphoma (DLBCL).
A. Venn diagram of overlapping miRNAs in GSE171272 and GSE173080. B. Correlation of miRNAs Between the GSE171272 and GSE173080 datasets based on trend agreement. The blue dots represent consistent trends, while the gray dots represent inconsistent trends. C. Venn diagram showing overlapping differentially expressed miRNAs in GSE171272 and GSE173080 with an adjusted *p*<0.05 and |logFC| > 1.5. D. Univariate Cox analysis of DLBCL patients from the TCGA database identifying 8 statistically significant miRNAs. E. Intersection of the differentially expressed miRNAs identified in GSE171272 with those that were statistically significant in the univariate Cox regression analysis of DLBCL patients from the TCGA database. F. Frequency of upregulation and downregulation of hsa-miR-23a-5p in tumor versus normal tissues across various cancers in the dbDEMC database. The numbers in the table represent the count of upregulated and downregulated hsa-miR-23a-5p in each tumor dataset. G. Survival analysis based on high and low expression groups of hsa-miR-23a-5p in DLBCL Patients from the TCGA database. H. Area under the time-dependent ROC curve for hsa-miR-23a-5p in DLBCL Patients from the TCGA Database.

Table 1. Basic characteristics of diffuse large B cell lymphoma patients.

Characteristics	Low group (N=24)	High group (N=23)	p
Age, years	56.25 ± 14.47	56.30 ± 14.03	0.992
Gender, %			0.891
Female	13 (54.17%)	12 (52.17%)	
Male	11 (45.83%)	11 (47.83%)	
Race/ethnicity, %			0.879
Asian	9 (37.50%)	9 (37.50%)	
white	15 (62.50%)	13 (56.53%)	
black or African American	0 (0.00%)	1 (4.35%)	
Clinical stage, %			0.510
Stage I	4 (19.05%)	3 (15.00%)	
Stage II	9 (42.86%)	8 (40.00%)	
Stage III	1 (4.76%)	4 (20.00%)	
Stage IV	7 (33.33%)	5 (25.00%)	
Primary therapy outcome, %			0.374
Complete Remission/Response	19 (82.61%)	15 (78.96%)	
Partial Remission/Response	2 (8.70%)	0 (0.00%)	
Stable Disease	1 (4.35%)	1 (5.26%)	
Progressive Disease	1 (4.35%)	3 (15.79%)	
Radiation therapy, %			0.348
No	19 (82.61%)	20 (95.24%)	
Yes	4 (17.39%)	1 (4.76%)	
Extranodal involvement, %			0.182
No	10 (45.45%)	15 (65.22%)	
Yes	12 (54.55%)	8 (34.78%)	
Follow up, years	3.10 ± 5.53	3.81 ± 4.19	0.815
Hsa-miR-23a-5p	0.36 ± 0.27	2.22 ± 1.05	<0.001
LDH level			0.016
Normal	3 (20.00%)	9 (64.29%)	
Unnormal	12 (80.00%)	5 (35.71%)	
Ki-67 (MIB-1) status			0.118
0 - 25%	0 (0.00%)	1 (9.09%)	
26 - 50%	3 (18.75%)	0 (0.00%)	
51 - 75%	5 (31.25%)	7 (63.64%)	
76 - 100%	8 (50.00%)	3 (27.27%)	

Mean±SD for continuous variable; (%) for categorical variables: the *p* value was calculated using the Kruskal Wallis rank sum test or Fisher exact test. LDH: lactate dehydrogenase; N: number; SD: standard deviation.
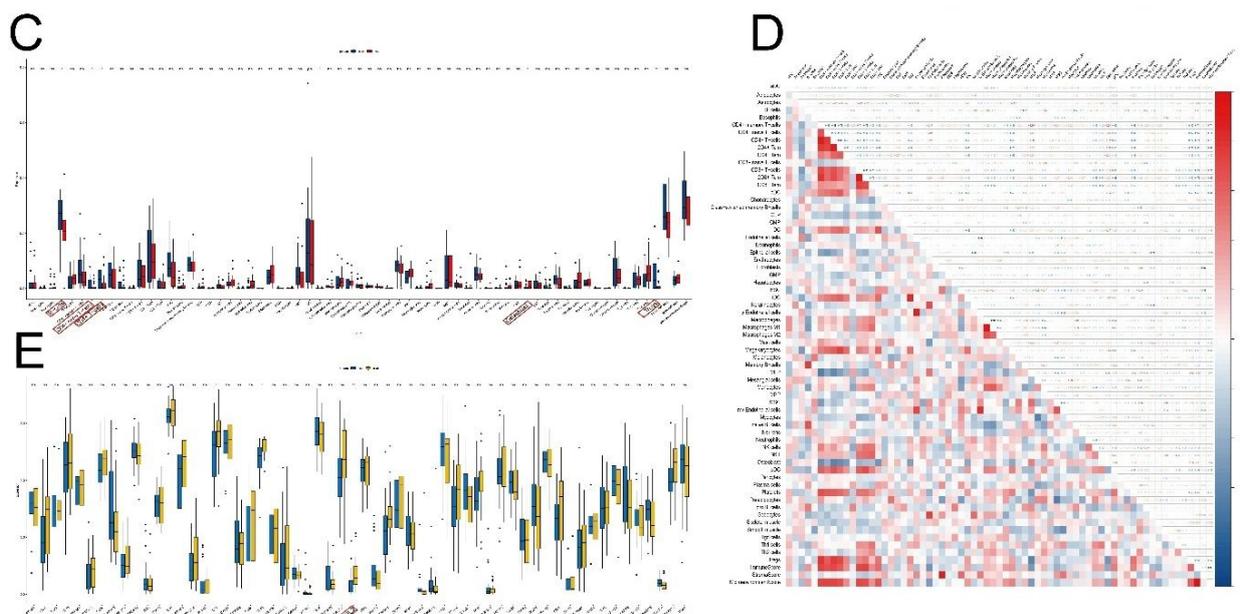
Table 2. Univariate and multivariate Cox proportional hazards model of hsa-miR-23a-5p in diffuse large B cell lymphoma patients.

Factors	Univariate		Multivariate	
	HR (95% CI)	p	HR (95% CI)	p
Age	1.30 (0.32, 5.27)	0.712	33.58 (0.48, 2340.18)	0.105
Gender	1.014 (0.24, 4.21)	0.985	3.27 (0.07, 159.96)	0.551
Race/ethnicity	0.56 (0.13, 2.45)	0.442	1.77 (0.04, 81.06)	NR
Clinical stage		0.897		0.463
Stage I	0.80 (0.05, 14.21)	0.878	0.23 (0.00, 750.69)	0.720
Stage II	0.59 (0.05, 6.88)	0.670	0.00 (0.00, 13.02)	0.151
Stage III	0.54 (0.03, 8.99)	0.666	0.01 (0.00, 23.3)	0.219
Stage IV	1.37 (0.13, 15.07)	0.797	0.75 (0.00, 1459.94)	0.941
Primary therapy outcome		0.0027		0.664
Complete Remission/Response	0.07 (0.01, 0.42)	0.004	0.01 (0.00, 15.17)	0.222
Partial Remission/Response	0.00 (0.00, NA)	0.991	0.00 (0.00, NA)	0.996
Stable Disease	0.00 (0.00, NA)	0.991	0.00 (0.00, NA)	0.992
Progressive Disease	0.75 (0.10, 5.76)	0.784	0.10 (0.00, 4653.20)	0.681
Radiation therapy	0.04 (0, 415.19)	0.493	0.00 (0.00, NA)	0.977
Extranodal involvement	1.01 (0.24, 4.29)	0.988	1.10 (0.00, 470.99)	0.975
Hsa-miR-23a-5p	1.73 (1.03, 2.89)	0.037	13.23 (1.32, 132.58)	0.028

CI: confidence interval; HR: hazard ratio; NA: not available; NR: not reported.

Figure 3. The landscape of tumor-infiltrating immune cells profile and immune-related genes analysis.
A. Barplot showing the proportion of 21 kinds of TICs in DLBCL tumor samples. B. The box plot illustrates the differential distribution of 21 types of immune cells between DLBCL tumor samples with low and high expression levels of hsa-miR-23a-5p, relative to the median expression level of hsa-miR-23a-5p. A Wilcoxon test was used to assess the significance of these differences. C. The box plot showed the differential distribution of 64 types of immune cells between DLBCL tumor samples with low and high expression levels of hsa-miR-23a-5p, relative to the median expression level of hsa-miR-23a-5p. A Wilcoxon test was used to assess the significance of these differences. D. Heatmap showing the correlation between 64 kinds of TICs and numeric in each tiny box indicating the correlation coefficient between two kinds of cells. The shade of each tiny color box represented the corresponding correlation value between two cells, and the Spearman coefficient was used for the significance test. E. The box plot showed the differential distribution of 58 types of immune-related genes between DLBCL tumor samples with low and high expression levels of hsa-miR-23a-5p, relative to the median expression level of hsa-miR-23a-5p. A Wilcoxon test was used to assess the significance of these differences. (ns, not significant; *p<0.05; **p<0.01; ***p<0.001; ****p<0.0001).
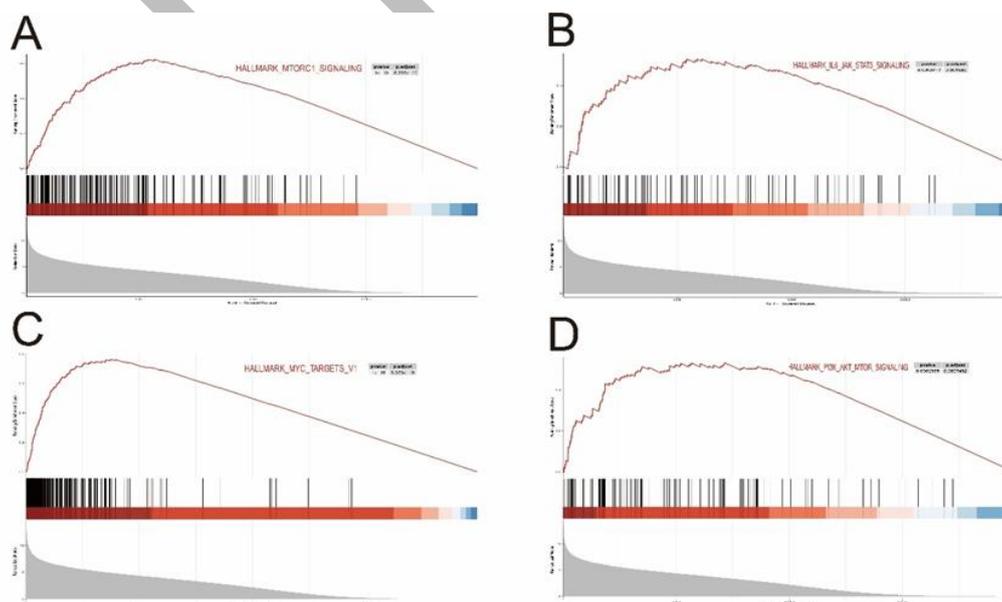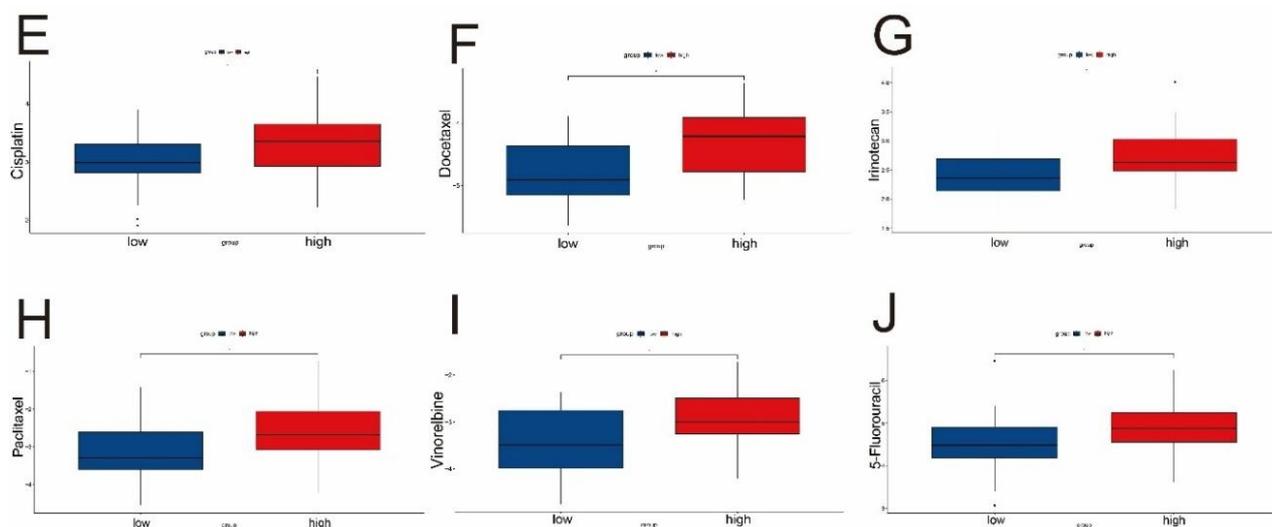
Figure 4. The landscape of gene set enrichment analysis and drug sensitivity analysis.
A–D. The enriched gene sets in the HALLMARK collection by the high hsa-miR-23a-5p expression sample. Up-regulated genes are located on the left, approaching the origin of the coordinates; by contrast, the down-regulated genes lie on the right of the x-axis. Only gene sets with adjusted *p*<0.05 were considered significant. And only several leading gene sets were displayed in the plot. E–J. The box plot illustrates the differential distribution of IC50 values for cisplatin, docetaxel, irinotecan, paclitaxel, vinorelbine, and 5-fluorouracil in DLBCL tumor samples with low and high expression levels of hsa-miR-23a-5p, compared to the median expression level of hsa-miR-23a-5p. (ns, not significant; *p*<0.05; **p*<0.01; ***p*<0.001; ****p*<0.0001).

Target Gene Analysis of hsa-miR-23a-5p

To further evaluate hsa-miR-23a-5p, miRNA-target prediction databases including TargetScan, miRWalk, and RNA22 were used to identify its target genes (Figure 5A). PPI networks were constructed for the target genes with an interaction score threshold of 0.9, and hub target genes were screened by MCC, MNC, DMNC, and Degree algorithms (Figure 5B, 5C) (Supplement Table 4). GO and KEGG pathway analyses were carried out on these hub genes. Experimentally validated miRNA-target interactions were retrieved from miRTarBase, DIANA-TarBase, and NPInter (Figure 5D) (Supplementary Table 5). Among the validated target genes, only one hub gene, *SNRPD1*, intersected with the hub target genes (Figure 5E). GO and KEGG analyses of the miRNA-target hub genes elucidated their involvement in ribonucleoprotein and rRNA-associated biological processes (Figure 5F–I). The process of ribonucleoprotein complex biogenesis in the GO enrichment results is crucial for cell proliferation,[25] while rRNA processing involves the generation and maturation of ribosomal RNA.[26] These processes are closely related to the rapid proliferation of DLBCL cells. In the KEGG pathways, The ribosome pathway plays a central role in protein synthesis, essential for cell

growth, and its dysregulation is closely associated with the development of various hematologic cancers.[27] The ribosome biogenesis in eukaryotes pathway involves the assembly and formation of ribosomes, and dysregulation of this pathway could promote tumorigenesis and facilitate tumor metastasis.[28] In summary, the GO and KEGG enrichment results reveal the key biological processes and pathways mediated by hsa-miR-23a-5p through the regulation of hub proteins. These mechanisms are central to the development and progression of DLBCL cells.

SNRPD1 Gene Mutation and Survival Analysis in TCGA and GSE31312 Datasets

We analyzed gene mutations in DLBCL patients from the TCGA database (Figure 6A). No mutations were detected in *SNRPD1* (Figure 6B). According to the median expression of *SNRPD1*, patients were stratified into high and low expression categories for survival and Cox univariate analysis (Figures 6C, D). Given the small sample size in the TCGA cohort, we further performed survival analysis, as well as both univariate and multivariate Cox analyses on the larger GSE31312 dataset, which also yielded statistically significant results (Figures 6E–G).
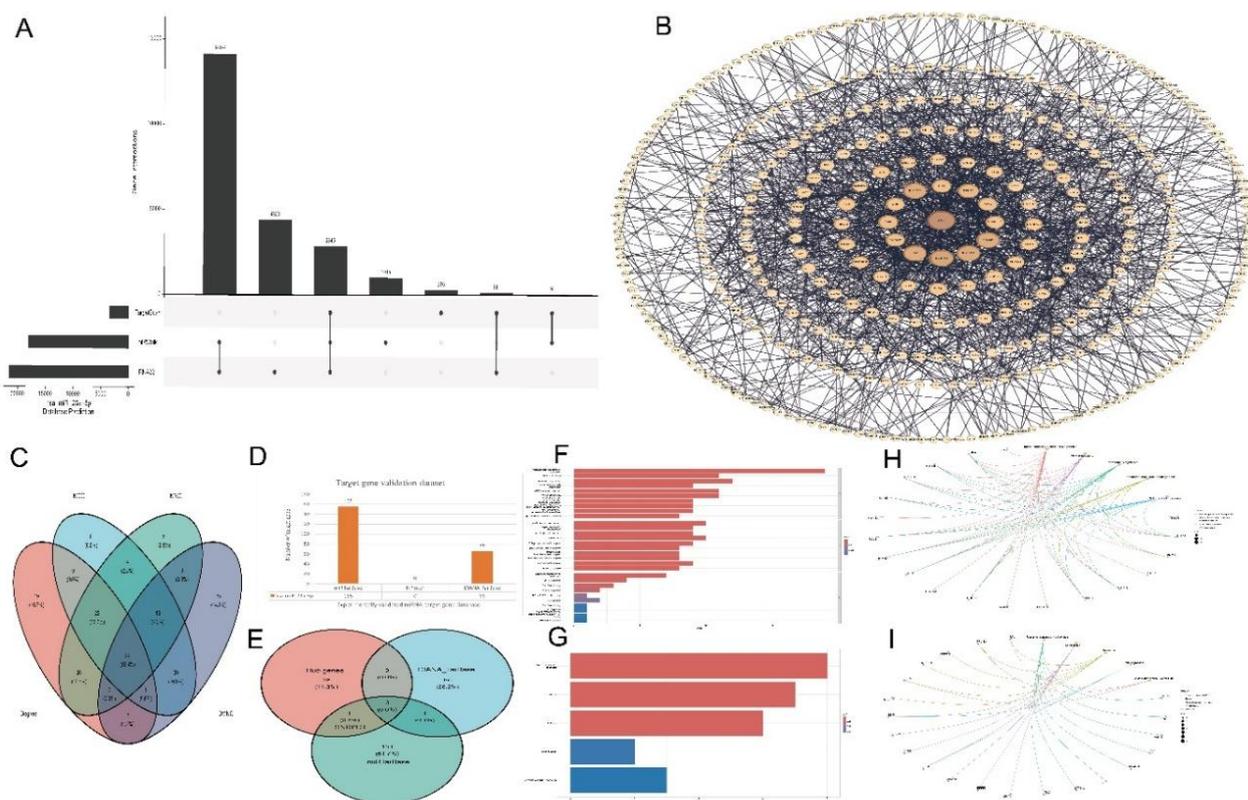
Figure 5. Analysis of hsa-miR-23a-5p targets. A. The upset plot of the hsa-miR-23a-5p target genes prediction database by TargetScan, miRWalk, RNA22. B. PPI networks with a 0.9 minimum required interaction score for the respective target genes of miRNAs. Only a subset of gene interactions with the highest degree rankings are displayed in the plot. C. Hub target genes screened by MCC, MNC, DMNC, and Degree algorithms. D. The number of hsa-miR-23a-5p target genes predicted by the miRTarBase, DIANA-TarBase, and NPInter databases. E. Intersection of hub target genes and experimentally validated target genes of hsa-miR-23a-5p. F. GO biological processes, cellular components, and molecular functions of the hsa-miR-23a-5p hub target genes. G. Analysis of the KEGG of the hsa-miR-23a-5p hub target genes. H, I. The specific mRNAs involved in the top five biological processes of GO and KEGG enrichment analysis.
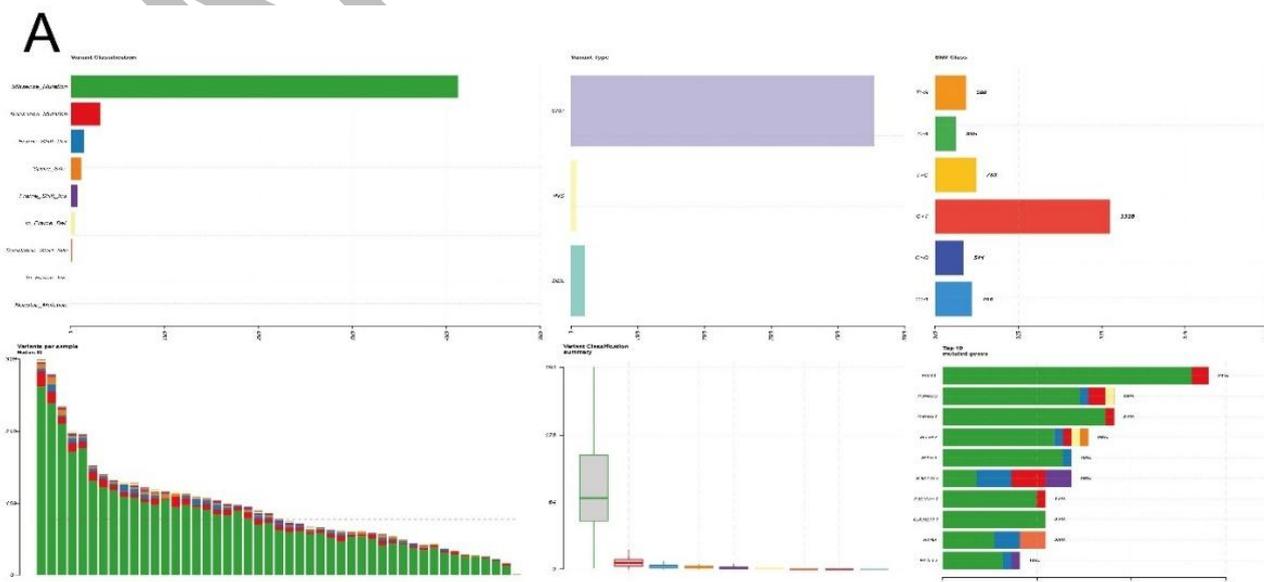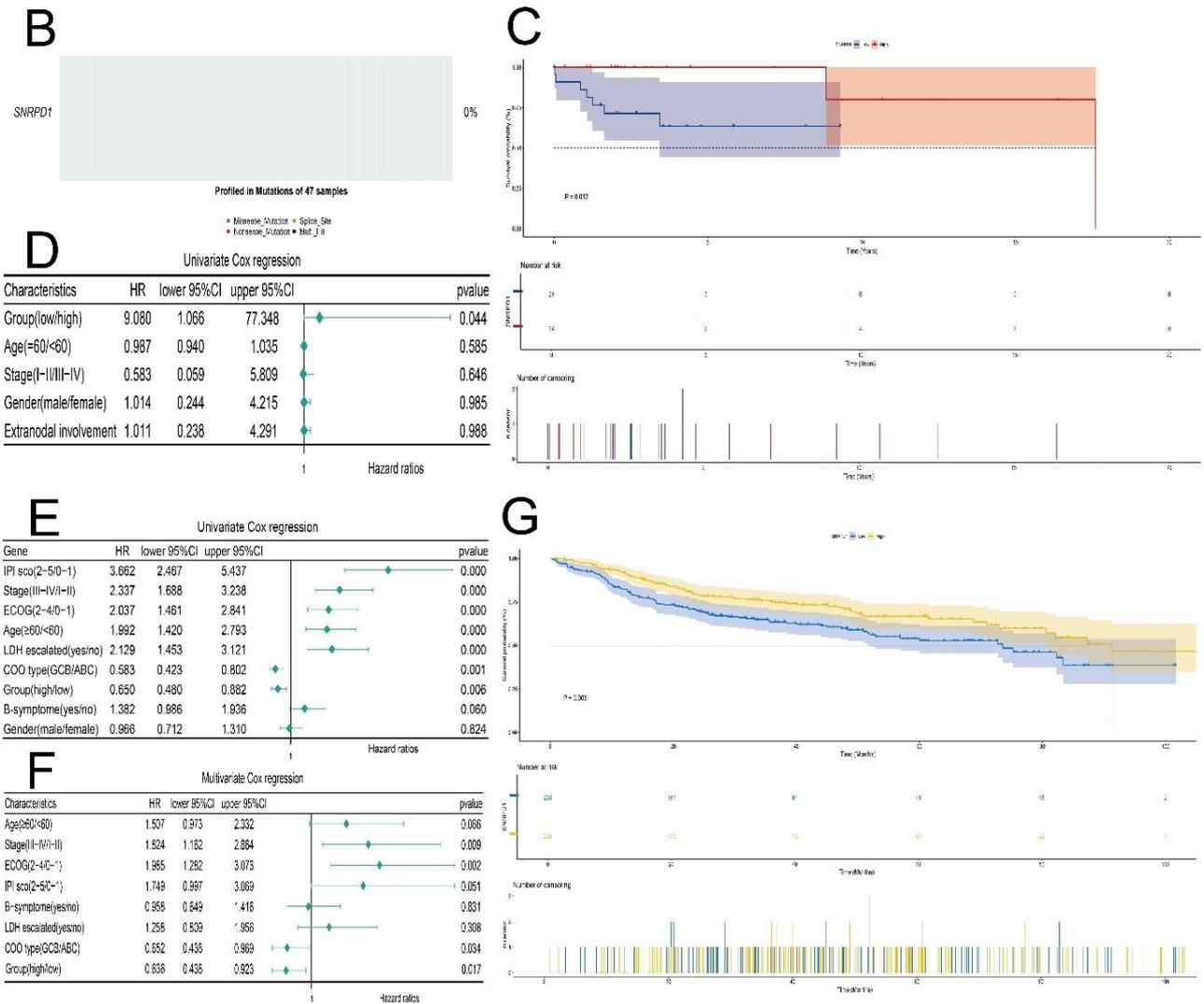
Figure 6. The landscape of somatic mutation profile, univariate and multivariate Cox regression analysis, and survival analysis of *SNRPD1*. A. Somatic mutation profile of DLBCL patients in the TCGA database. B. The somatic mutation profile of *SNRPD1* in 47 DLBCL patients from the TCGA database. C. Survival analysis based on the expression of *SNRPD1* categorized into high and low groups compared to the median expression level in 47 DLBCL patients from the TCGA database. D. Forest plot showing that the signature is significantly associated with prognosis in 47 DLBCL patients from the TCGA database. E, F. The forest plot shows that the signature is significantly associated with prognosis and operates independently of all clinical features in both univariate and multivariate Cox proportional hazards regression analyses in the GSE31312 dataset. G. Survival analysis based on the expression of *SNRPD1* categorized into high and low groups compared to the median expression level in 470 DLBCL patients from the GSE31312 database.

DISCUSSION

This research demonstrated that hsa-miR-23a-5p is associated with prognostic outcomes, immune landscapes, chemoresistance, and biological processes in TCGA DLBCL patients, positioning it as a potential risk factor. Conversely, its target gene *SNRPD1* is associated with a favorable prognosis and appears to function as a protective factor. Importantly, hsa-miR-23a-5p is significantly overexpressed in both serum exosomes and tumor tissues of DLBCL patients, highlighting its potential as a biomarker and suggesting

its utility for non-invasive liquid biopsy strategies in clinical assessment.

To our knowledge, this study provides the first comprehensive evidence linking hsa-miR-23a-5p to DLBCL pathogenesis and prognosis through integrated analysis both tumor tissues and serum-derived exosomes. MiRNAs play an essential role in regulating cellular processes and are critical post-transcriptional regulators of gene expression.[29] Among the various biomolecules associated with tumors, exosomal miRNAs are considered particularly promising. MiRNAs can be easily extracted from bodily fluids through noninvasive procedures and analyzed using qRT-PCR, making them highly valuable for cancer diagnosis and prognosis.[30–33] To translate these findings into clinical practice, hsa-miR-23a-5p could be developed as a non-invasive biomarker for patient stratification, monitoring treatment response, and predicting prognosis in DLBCL. By measuring exosomal has-miR-23a-5p levels in blood or serum, clinicians can identify immune subtypes, guide immune therapy or chemotherapy decisions, and monitor treatment efficacy. Further validation in large-scale clinical trials and the development of standardized assays will be essential for its integration into routine clinical practice.

Circulating tumor DNA (ctDNA), circulating tumor cells (CTCs), and exosomes are major analytes in liquid biopsy.[34] Among them, exosomes outperform CTCs and ctDNA in liquid biopsies. Exosomes are present in millions per milliliter in biological fluids, making them more accessible compared to the few CTCs found per milliliter of blood sample.[35–37] Additionally, exosomes carry significant biological information derived from their parent cells and are produced by live cells,[37,38] making them more representative than ctDNA, which is largely shed from apoptotic or dead tumor cells. Furthermore, serum exosomes contain higher miRNA concentrations than ctDNA, making them more suitable for blood-based miRNA omics studies. Serum exosomes may be more protected from degradation, allowing for a more precise distribution of target cells in the blood samples.[39] Thus, exosomes offer significant advantages for fluid monitoring in patients with tumors. However, the high heterogeneity and nanoscale size of exosomes present significant technical challenges in understanding their molecular interactions and information.[34]

Current detection methods for miRNAs include quantitative polymerase chain reaction (qPCR),

microarray analysis, next-generation sequencing (NGS), northern blotting, in situ hybridization (ISH), droplet digital polymerase chain reaction (ddPCR), and biosensors. Among these, qPCR is widely used due to its high sensitivity and specificity.[40] In contrast, microarray analysis is less sensitive for low-abundance miRNAs but can profile multiple miRNAs simultaneously, making it suitable for broad analyses.[41] NGS, such as RNA sequencing(RNA-seq), offer high throughput and can identify novel miRNAs, but they are costly.[42,43] Northern blotting is suitable for miRNA-specific detection;[44] ISH requires tissue samples;[45] Although ddPCR is highly sensitive and precise but has limited multiplexing capability;[46] and biosensors allow real-time monitoring but are prone to interference.[47] Taken together, qPCR is better suited for clinical detection of miRNAs, with a relatively straightforward workflow that supports rapid and accurate testing in clinical settings.

Hsa-miR-23a possesses two mature bodies, hsa-miR-23a-3p and hsa-miR-23a-5p. In the present study, we discovered that hsa-miR-23a-5p was overexpressed in both tumor tissues and serum exosomes, whereas hsa-miR-23a-3p showed no significant changes. This aligns with previous studies identifying hsa-miR-23a-5p as an oncogene involved in cell proliferation, migration, and apoptosis.[48] Numerous studies have investigated hsa-miR-23a-5p levels in different diseases, such as non-small cell lung cancer lymph node metastasis,[49] osteolytic diseases,[50] severe sepsis,[51] hepatocellular carcinoma,[52] and acute myeloid leukemia.[53] It is also upregulated in bladder cancer[48] and esophageal squamous cell carcinoma.[54] Squadrito et al found that changes in miRNA expression in cell correspond to similar trends in exosomal miRNAs, though the magnitude of the change was greater.[55] MiRNAs are post-transcriptional regulators that negatively affect translation. According to DLBCL relevant studies, miR-21, miR-155, miR-187, miR-10a, miR-26a, miR-27b, and miR-224 promote the progression through various mechanisms;[56–62] genes such as miR-155, miR-146a, miR-200c, miR-18a, and miR-222 are linked to prognosis;[63–66] additionally, miR-21, miR-34a, miR-181a, miR-370-3p, miR-381-3p, and miR-409-3p are associated with drug resistance.[66–69] Furthermore, apart from its correlation with prognosis and drug resistance, the mechanism of hsa-miR-23a-5p is more closely related to the immune microenvironment, providing it with a distinct advantage. In the multivariate analysis,

we identified hsa-miR-23a-3p as an independent prognostic factor for DLBCL, with a hazard ratio of 13.23 (CI: 1.32–132.58). However, due to the relatively small sample size in this study, the wide confidence intervals observed may reflect increased variability in the hazard ratio estimates. Given the observed instability, we interpret our findings with caution. Although the association between hsa-miR-23a-3p and DLBCL appears promising, we acknowledge that these conclusions need to be validated in larger, independent cohorts to confirm their robustness. Moreover, the absence of important clinical variables-such as double-hit/triple-hit status, *MYC/BCL2/BCL6* rearrangements, and treatment regimens-represents a limitation of the Cox proportional hazards model used in this study. These factors are key prognostic markers in DLBCL, and their inclusion in future research will be crucial for fully validating and enhancing the clinical applicability of miRNA biomarkers. Through survival analysis, univariate, and multivariate analyses at the mRNA level, we identified *SNRPD1* as a protective factor. Upregulation of hsa-miR-23a-5p suppress *SNRPD1* translation, ultimately resulting in worsened prognosis for patients (Figures 6C, G).[29,70]

Our analyses indicate that hsa-miR-23a-5p fosters an immunosuppressive microenvironment conducive to DLBCL progression. CIBERSORT analysis revealed that the high expression group of hsa-miR-23a-5p exhibited a lower proportion of activated NK cells and a higher proportion of resting mast cells. The low proportions of activated NK cells and increased resting mast cells together promote immune suppression, accelerating tumor growth. In the xCell analysis, the high expression group of hsa-miR-23a-5p was associated with reduced infiltration of CD4^{+} naive T cells, B cells, CD4^{+} T cells, and Tregs, reflecting immune escape and promote tumor proliferation. Based on paired RNA-Seq and miRNA-Seq experiments, it was found that hsa-miR-23a-5p is a critical miRNA involved in the polarization of M2 macrophages, potentially modulating immune responses by driving their polarization.[71] M2 macrophages play an immunosuppressive role in the tumor microenvironment by secreting anti-inflammatory cytokines, which promote tumor growth and immune evasion.[72] The numbers of activated NK cells, resting mast cells, CD4^{+} naive T cells, B cells, CD4^{+} T cells, and Tregs are closely associated with the polarization of M2 macrophages.[73] Hsa-miR-23a-5p may promote the polarization of M2 macrophages, thereby modulating the tumor immune microenvironment and promoting immune suppression, which subsequently influences the activity of various immune cell populations. Inhibiting the expression of hsa-miR-23a-5p could also impede M2 macrophage polarization, thereby affecting the activity of NK cells, mast cells, Tregs, and other immune cells. This effect may offer potential therapeutic strategies for tumor immunotherapy. However, these findings still require experimental validation. Additionally, the high-expression group of hsa-miR-23a-5p showed higher levels of keratinocytes and osteoblasts, both linked to tumor growth.[74,75]

In the immune-related molecule analysis, we noted that *BTNL2* expression was upregulated in the group with high expression of hsa-miR-23a-5p. *BTNL2* suppresses effector T cell activity, leading to immune suppression. Butyrophilin-like protein 2 (BTNL2) is a transmembrane immunoregulatory protein that suppresses the anti-tumor immune response by interacting with γδ T cells to promote IL-17A production in the tumor microenvironment, enhancing immune resistance. Studies have shown that blocking *BTNL2* in animal models significantly inhibits tumor growth and extends survival, with a synergistic effect when combined with anti-PD-1 treatment. Inhibiting *BTNL2* also reduces myeloid-derived suppressor cell accumulation, promoting CD8^{+} T cell infiltration. *BTNL2* plays a key role in immune evasion, and its inhibition, combined with anti-PD-1/PD-L1 blockade, shows promise for tumors that are resistant to anti-PD-1 therapy, potentially offering new immunotherapy options for "cold" tumors.[76]

Recent research has emphasized the crucial role of exosomes in cell-to-cell communication during cancer progression.[77] Exosomes can facilitate tumor escape by creating an immunosuppressive microenvironment that favors tumor development, invasion, and metastasis.[78] The communication between cancer cells and their microenvironment significantly influences chemoresistance, survival, proliferation, migration, and resistance to apoptosis, which drives the progression of various hematologic malignancies.[79] Furthermore, this interaction helps cancer cells evade immune surveillance and establish an immunosuppressive microenvironment, thereby advancing tumor progression.[80,81] These interactions can occur through the release of exosomes, the secretion of soluble substances, or direct interaction between cells.[79]

Increasing evidence suggests that exosomal miRNAs can actively modulate the immune microenvironment.[82] Previous research has revealed that exosomes derived from tumors contribute to tumor progression by releasing pro-inflammatory cytokines, promoting neutrophil infiltration through Toll-like receptor 3 activation, enhancing angiogenesis, and attracting myeloid-derived suppressor cells.[83] Moreover, tumor-associated miRNAs selectively target critical genes involved in immune suppression, angiogenesis, and epithelial-mesenchymal transition, thus preparing the pre-metastatic niche in distant organs.[84]

Additionally, GSEA revealed that the genes in the high-expression group of hsa-miR-23a-5p were predominantly enriched in pathways such as MTORC1, IL6-JAK-STAT3, MYC, and PI3K-AKT-MTOR, all associated with tumor proliferation. As tumor proliferation increases, resistance to chemotherapy drugs also increases. Consequently, the high-expression group of hsa-miR-23a-5p exhibited higher IC_{50} values for drugs such as cisplatin, docetaxel, irinotecan, paclitaxel, vinorelbine, and 5-fluorouracil. Based on the negative regulation of target genes by miRNAs, we observed that the low expression group of *SNRPD1* had a poorer prognosis, further indirectly validating the role of hsa-miR-23a-5p as a risk factor. Taken together, these pieces of evidence suggest that hsa-miR-23a-5p is strongly linked to tumor growth and adverse prognosis.

This study had several strengths, including the use of patient data from multiple datasets and careful sample selection, which enhance the reliability and confidence of the results. However, our study also has several significant limitations. Firstly, it currently lacks functional validation, including in vitro and in vivo experiments, which limits our understanding of the biological function and mechanistic role of hsa-miR-23a-5p in tumor progression. To address this, future studies should incorporate experimental validation, including cell-based assays, xenograft models, and in vivo studies. In addition, DLBCL patients should be recruited for monitoring and follow-up of peripheral blood exosome hsa-miR-23a-5p levels. Moreover, the low prevalence of lymphoma resulted in a relatively small sample size for each dataset, which could have contributed to the observed instability in the hazard ratios. Limited sample sizes can also limit statistical power and reproducibility, increasing variability in detecting true effects. To enhance reproducibility, we plan to expand the sample size in future studies, ensuring

that the results are more robust and consistently validated across different datasets. Additionally, as the datasets were derived from various databases, with miRNA data from tissue and serum exosomes of different patients, it was challenging to establish a direct correlation between serum exosomal miRNAs and tissue miRNAs. Furthermore, due to limitations in miRNA detection platforms, many datasets examining miRNAs in DLBCL patients did not distinguish between hsa-miR-23a-5p and hsa-miR-23a-3p, resulting in a limited number of datasets available for inclusion. One additional limitation of this study is the reliance on retrospective data, which may introduce biases and limit the ability to fully capture the clinical heterogeneity and real-world applicability of the findings. Finally, due to data limitations, we were unable to include data on all the factors affecting DLBCL. Nonetheless, the existing association between hsa-miR-23a-5p and DLBCL remains robust enough to indicate that it is unlikely to be greatly affected by unaccounted-for variables.

In summary, this study identifies hsa-miR-23a-5p and its target *SNRPD1* as promising potential prognostic factors for DLBCL. Specifically, the overexpression of hsa-miR-23a-5p in serum exosomes of DLBCL patients may provide a convenient and non-invasive approach for the clinical evaluation of DLBCL. However, further research and validation are necessary to confirm these findings.

STATEMENT OF ETHICS

The portions of this study involving human participants, human material, and human data were obtained from the GEO and TCGA public databases. This study was based on open-source data and did not involve human or animal experimentation; therefore, no additional ethical approval was required.

FUNDING

CONFLICT OF INTEREST

The authors declare no conflicts of interest.

ACKNOWLEDGMENTS

We would like to express our sincere gratitude to all the participants in this study and extend our appreciation to the GEO and TCGA databases for providing their platforms, as well as to the contributors who uploaded their valuable datasets.

DATA AVAILABILITY

The dataset from this study is available in the GEO (https://www.ncbi.nlm.nih.gov/) repository under the accession codes GSE173080, GSE171272, and GSE31312. TargetScan (https://www.targetscan.org/vert_80/), miRWalk (http://mirwalk.umm.uni-heidelberg.de/), RNA22 (https://cm.jefferson.edu/rna22/), miRTarBase (https://mirtarbase.cuhk.edu.cn/), DIANA-TarBase(http://diana.imis.athena-innovation.gr/), and NPInter (http://bigdata.ibp.ac.cn/npinter4) were used in this study. Transcribed gene expression and clinical data, including mature miRNAs from DLBCL patients, are available in the TCGA database (https://portal.gdc.cancer.gov/).

AI ASSISTANCE DISCLOSURE

No AI tools were used in preparing this manuscript.

REFERENCES

1. Sehn LH, Salles G. Diffuse large B-cell lymphoma. N Engl J Med. 2021;384(9):842-58.

2. Alizadeh AA, Eisen MB, Davis RE, et al. Distinct types of diffuse large B-cell lymphoma identified by gene expression profiling. Nature. 2000;403(6769):503-11.

3. Schmitz R, Wright GW, Huang DW, et al. Genetics and pathogenesis of diffuse large B-cell lymphoma. N Engl J Med. 2018;378(15):1396-407.

4. Bea S, Zettl A, Wright G, et al. Diffuse large B-cell lymphoma subgroups have distinct genetic profiles that influence tumor biology and improve gene-expression-based survival prediction. Blood. 2005;106(9):3183-90.

5. Chapuy B, Stewart C, Dunford AJ, et al. Molecular subtypes of diffuse large B cell lymphoma are associated with distinct pathogenic mechanisms and outcomes. Nat Med. 2018;24(5):679-90.

6. Tilly H, Morschhauser F, Sehn LH, et al. Polatuzumab vedotin in previously untreated diffuse large B-cell lymphoma. N Engl J Med. 2022;386(4):351-63.

7. Meyer PN, Fu K, Greiner TC, et al. Immunohistochemical methods for predicting cell of origin and survival in patients with diffuse large B-cell lymphoma treated with rituximab. J Clin Oncol. 2011;29(2):200-7.

8. National Cancer Institute. Diffuse Large B-Cell Lymphoma-Cancer Stat Facts. SEER. Accessed April 24, 2024.https://seer.cancer.gov/statfacts/html/dlbcl.html

9. Bouroumeau A, Bussot L, Bonnefoix T, et al. c-MYC and p53 expression highlight starry-sky pattern as a favourable prognostic feature in R-CHOP-treated diffuse large B-cell lymphoma. J Pathol Clin Res. 2021;7(6):604-15.

10. Vodicka P, Klener P, Trneny M. Diffuse large B-cell lymphoma (DLBCL): early patient management and emerging treatment options. Onco Targets Ther. 2022;15:1481-501.

11. Jiang S, Qin Y, Jiang H, et al. Molecular profiling of Chinese R-CHOP treated DLBCL patients: identifying a high-risk subgroup. Int J Cancer. 2020;147(9):2611-20.

12. Lim KG, Sumera A, Burud IAS, Venkateswaran SP. Diffuse large B-cell lymphoma research in Malaysia: a review. Malays J Pathol. 2023;45(1):1-10.

13. Morin RD, Assouline S, Alcaide M, et al. Genetic landscapes of relapsed and refractory diffuse large B-cell lymphomas. Clin Cancer Res. 2016;22(9):2290-300.

14. Shimkus G, Nonaka T. Molecular classification and therapeutics in diffuse large B-cell lymphoma. Front Mol Biosci. 2023;10:1124360.

15. Zhang J, Gu Y, Chen B. Drug-resistance mechanism and new targeted drugs and treatments of relapse and refractory DLBCL. Cancer Manag Res. 2023;15:245-55.

16. Wight JC, Chong G, Grigg AP, Hawkes EA. Prognostication of diffuse large B-cell lymphoma in the molecular era: moving beyond the IPI. Blood Rev. 2018;32(5):400-15.

17. Lee YS, Dutta A. MicroRNAs in cancer. Annu Rev Pathol. 2009;4:199-227.

18. Chen Y, Stallings RL. Differential patterns of microRNA expression in neuroblastoma are correlated with prognosis, differentiation, and apoptosis. Cancer Res. 2007;67(3):976-83.

19. Scott GK, Goga A, Bhaumik D, et al. Coordinate suppression of ERBB2 and ERBB3 by enforced expression of micro-RNA miR-125a or miR-125b. J Biol Chem. 2007;282(2):1479-86.

20. Kosaka N, Yoshioka Y, Fujita Y, Ochiya T. Versatile roles of extracellular vesicles in cancer. J Clin Invest. 2016;126(4):1163-72.

21. Raposo G, Nijman HW, Stoorvogel W, et al. B lymphocytes secrete antigen-presenting vesicles. J Exp Med. 1996;183(3):1161-72.

22. uang X, Yuan T, Tschannen M, et al. Characterization of human plasma-derived exosomal RNAs by deep sequencing. BMC Genomics. 2013;14:319.

23. Li C, Zhou T, Chen J, et al. The role of exosomal miRNAs in cancer. J Transl Med. 2022;20(1):6.

24. Cao D, Cao X, Jiang Y, et al. Circulating exosomal microRNAs as diagnostic and prognostic biomarkers in patients with diffuse large B-cell lymphoma. Hematol Oncol. 2022;40(2):172-80.

25. Jiao L, Liu Y, Yu XY, et al. Ribosome biogenesis in disease: new players and therapeutic targets. Signal Transduct Target Ther. 2023;8(1):15.

26. Gaviraghi M, Vivori C, Tonon G. How cancer exploits ribosomal RNA biogenesis: a journey beyond the boundaries of rRNA transcription. Cells. 2019;8(9):1069.

27. Elhamamsy AR, Metge BJ, Alsheikh HA, et al. Ribosome biogenesis: a central player in cancer metastasis and therapeutic resistance. Cancer Res. 2022;82(13):2344-53.

28. Hwang SP, Denicourt C. The impact of ribosome biogenesis in cancer: from proliferation to metastasis. NAR Cancer. 2024;6(2):zcae017.

29. Krol J, Loedige I, Filipowicz W. The widespread regulation of microRNA biogenesis, function and decay. Nat Rev Genet. 2010;11(9):597-610.

30. Manier S, Liu CJ, Avet-Loiseau H, et al. Prognostic role of circulating exosomal miRNAs in multiple myeloma. Blood. 2017;129(17):2429-36.

31. van Eijndhoven MA, Zijlstra JM, Groenewegen NJ, et al. Plasma vesicle miRNAs for therapy response monitoring in Hodgkin lymphoma patients. JCI Insight. 2016;1(19):e89631.

32. Lai X, Wang M, McElyea SD, et al. A microRNA signature in circulating exosomes is superior to exosomal glypican-1 levels for diagnosing pancreatic cancer. Cancer Lett. 2017;393:86-93.

33. Melo SA, Luecke LB, Kahlert C, et al. Glypican-1 identifies cancer exosomes and detects early pancreatic cancer. Nature. 2015;523(7559):177-82.

34. Siravegna G, Marsoni S, Siena S, Bardelli A. Integrating liquid biopsies into the management of cancer. Nat Rev Clin Oncol. 2017;14(9):531-48.

35. Cohen SJ, Punt CJ, Iannotti N, et al. Relationship of circulating tumor cells to tumor response, progression-free survival, and overall survival in patients with metastatic colorectal cancer. J Clin Oncol. 2008;26(19):3213-21.

36. Krebs MG, Sloane R, Priest L, et al. Evaluation and prognostic significance of circulating tumor cells in patients with non-small-cell lung cancer. J Clin Oncol. 2011;29(12):1556-63.

37. Cai X, Janku F, Zhan Q, Fan JB. Accessing genetic information with liquid biopsies. Trends Genet. 2015;31(10):564-75.

38. Hoshino A, Costa-Silva B, Shen TL, et al. Tumour exosome integrins determine organotropic metastasis. Nature. 2015;527(7578):329-35.

39. Yu W, Hurley J, Roberts D, et al. Exosome-based liquid biopsies in cancer: opportunities and challenges. Ann Oncol. 2021;32(4):466-77.

40. Voss G, Edsjö A, Bjartell A, Ceder Y. Quantification of microRNA editing using two-tailed RT-qPCR for improved biomarker discovery. RNA. 2021;27(11):1412-24.

41. Ekiz Kanik F, Celebi I, Sevenler D, et al. Attomolar sensitivity microRNA detection using real-time digital microarrays. Sci Rep. 2022;12(1):16220.

42. Benesova S, Kubista M, Valihrach L. Small RNA-sequencing: approaches and considerations for miRNA analysis. Diagnostics (Basel). 2021;11(6):1069.

43. Ergin S, Kherad N, Alagoz M. RNA sequencing and its applications in cancer and rare diseases. Mol Biol Rep. 2022;49(3):2325-33.

44. Yaylak B, Akgül B. Experimental microRNA detection methods. Methods Mol Biol. 2022;2257:33-55.

45. Paulsen IW, Bzorek M, Olsen J, et al. A novel approach for microRNA in situ hybridization using locked nucleic acid probes. Sci Rep. 2021;11(1):4504.

46. Cirillo PDR, Margiotti K, Mesoraca A, Giorlandino C. Quantification of circulating microRNAs by droplet digital PCR for cancer detection. BMC Res Notes. 2020;13(1):351.

47. Low SS, Ji D, Chai WS, et al. Recent progress in nanomaterials modified electrochemical biosensors for the detection of microRNA. Micromachines (Basel). 2021;12(11):1359.

48. Li Y, Quan J, Pan X, et al. Suppressing cell growth and inducing apoptosis by inhibiting miR-23a-5p in human bladder cancer. Mol Med Rep. 2018;18(6):5256-60.

49. Xu L, Li L, Li J, et al. Overexpression of miR-1260b in non-small cell lung cancer is associated with lymph node metastasis. Aging Dis. 2015;6(6):478-85.

50. Ma Y, Shan Z, Ma J, et al. Validation of downregulated microRNAs during osteoclast formation and osteoporosis progression. Mol Med Rep. 2016;13(3):2273-80.

51. Caserta S, Kern F, Cohen J, et al. Circulating plasma microRNAs can differentiate human sepsis and systemic inflammatory response syndrome (SIRS). Sci Rep. 2016;6:28006.

52. Zhao Y, Liu J, Xiong Z, et al. Exosome-derived miR-23a-5p inhibits HCC proliferation and angiogenesis by regulating PRDX2 expression: miR-23a-5p/PRDX2 axis in HCC progression. Heliyon. 2024;10(1):e23168.

53. Ganesan S, Palani HK, Lakshmanan V, et al. Stromal cells downregulate miR-23a-5p to activate protective autophagy in acute myeloid leukemia. Cell Death Dis. 2019;10(10):736.

54. Niwa Y, Yamada S, Sonohara F, et al. Identification of a serum-based miRNA signature for response of esophageal squamous cell carcinoma to neoadjuvant chemotherapy. J Transl Med. 2019;17(1):1.

55. Squadrito ML, Baer C, Burdet F, et al. Endogenous RNAs modulate microRNA sorting to exosomes and transfer to acceptor cells. Cell Rep. 2014;8(5):1432-1446.

56. Huang X, Shen Y, Liu M, et al. Quantitative proteomics reveals that miR-155 regulates the PI3K-AKT pathway in diffuse large B-cell lymphoma. Am J Pathol. 2012;181(1):26-33.

57. Liu K, Du J, Ruan L. MicroRNA-21 regulates the viability and apoptosis of diffuse large B-cell lymphoma cells by upregulating B cell lymphoma-2. Exp Ther Med. 2017;14(5):4489-96.

58. Fan Q, Meng X, Liang H, et al. miR-10a inhibits cell proliferation and promotes cell apoptosis by targeting BCL6 in diffuse large B-cell lymphoma. Protein Cell. 2016;7(12):899-912.

59. Huang F, Jin Y, Wei Y. MicroRNA-187 induces diffuse large B-cell lymphoma cell apoptosis via targeting BCL6. Oncol Lett. 2016;11(4):2845-50.

60. Jia YJ, Liu ZB, Wang WG, et al. HDAC6 regulates microRNA-27b that suppresses proliferation, promotes apoptosis and target MET in diffuse large B-cell lymphoma. Leukemia. 2018;32(3):703-11.

61. Song G, Song G, Ni H, et al. Deregulated expression of miR-224 and its target gene: CD59 predicts outcome of diffuse large B-cell lymphoma patients treated with R-CHOP. Curr Cancer Drug Targets. 2014;14(7):659-70.

62. Farina FM, Inguscio A, Kunderfranco P, et al. MicroRNA-26a/cyclin-dependent kinase 5 axis controls proliferation, apoptosis and in vivo tumor growth of diffuse large B-cell lymphoma cell lines. Cell Death Dis. 2017;8(6):e2890.

63. Wu X, Wang F, Li Y, et al. Evaluation of latent membrane protein 1 and microRNA-155 for the prognostic prediction of diffuse large B cell lymphoma. Oncol Lett. 2018;15(6):9725-34.

64. Zhong H, Xu L, Zhong JH, et al. Clinical and prognostic significance of miR-155 and miR-146a expression levels in formalin-fixed/paraffin-embedded tissue of patients with diffuse large B-cell lymphoma. Exp Ther Med. 2012;3(5):763-70.

65. Berglund M, Hedström G, Amini RM, et al. High expression of microRNA-200c predicts poor clinical outcome in diffuse large B-cell lymphoma. Oncol Rep. 2013;29(2):720-4.

66. Alencar AJ, Malumbres R, Kozloski GA, et al. MicroRNAs are independent predictors of outcome in diffuse large B-cell lymphoma patients treated with R-CHOP. Clin Cancer Res. 2011;17(12):4125-35.

67. Bai H, Wei J, Deng C, et al. MicroRNA-21 regulates the sensitivity of diffuse large B-cell lymphoma cells to the CHOP chemotherapy regimen. Int J Hematol. 2013;97(2):223-31.

68. Zhang Y, Guo CC, Guan DH, et al. Prognostic value of microRNA-224 in various cancers: a meta-analysis. Arch Med Res. 2017;48(5):472-82.

69. Leivonen SK, Icay K, Jäntti K, et al. MicroRNAs regulate key cell survival pathways and mediate chemosensitivity during progression of diffuse large B-cell lymphoma. Blood Cancer J. 2017;7(12):654.

70. Ha M, Kim VN. Regulation of microRNA biogenesis. Nat Rev Mol Cell Biol. 2014;15(8):509-24.

71. Lu L, McCurdy S, Huang S, et al. Time series miRNA-mRNA integrated analysis reveals critical miRNAs and targets in macrophage polarization. Sci Rep. 2016;6:37446.

72. Li M, Yang Y, Xiong L, et al. Metabolism, metabolites, and macrophages in cancer. J Hematol Oncol. 2023;16(1):80.

73. Xu Y, Wang X, Liu L, et al. Role of macrophages in tumor progression and therapy (Review). Int J Oncol. 2022;60(5):116.

74. Dainese-Marque O, Garcia V, Andrieu-Abadie N, Riond J. Contribution of keratinocytes in skin cancer initiation and progression. Int J Mol Sci. 2024;25(16):8894.

75. Logothetis CJ, Lin SH. Osteoblasts in prostate cancer metastasis to bone. Nat Rev Cancer. 2005;5(1):21-28.

76. Du Y, Peng Q, Cheng D, et al. Cancer cell-expressed BTNL2 facilitates tumour immune escape via engagement with IL-17A-producing γδ T cells. Nat Commun. 2022;13(1):231.

77. Li Y, You J, Zou Z, et al. Decoding the tumor microenvironment: exosome-mediated macrophage

polarization and therapeutic frontiers. Int J Biol Sci. 2025;21(9):4187-214.

78. Xie QH, Zheng JQ, Ding JY, et al. Exosome-mediated immunosuppression in tumor microenvironments. Cells. 2022;11(12):1948.

79. Dubois N, Crompot E, Meuleman N, et al. Importance of crosstalk between chronic lymphocytic leukemia cells and the stromal microenvironment: direct contact, soluble factors, and extracellular vesicles. Front Oncol. 2020;10:1422.

80. Witkowski MT, Dolgalev I, Evensen NA, et al. Extensive remodeling of the immune microenvironment in B cell acute lymphoblastic leukemia. Cancer Cell. 2020;37(6):867-82.e12.

81. Gargiulo E, Paggetti J, Moussay E. Hematological malignancy-derived small extracellular vesicles and tumor microenvironment: the art of turning foes into friends. Cells. 2019;8(5):498.

82. Nail HM, Chiu CC, Leung CH, et al. Exosomal miRNA-mediated intercellular communications and immunomodulatory effects in tumor microenvironments. J Biomed Sci. 2023;30(1):69.

83. Bardi GT, Smith MA, Hood JL. Melanoma exosomes promote mixed M1 and M2 macrophage polarization. Cytokine. 2018;105:63-72.

84. Bayat M, Sadri Nahand J. Exosomal miRNAs: the tumor's trojan horse in selective metastasis. Mol Cancer. 2024;23(1):167.